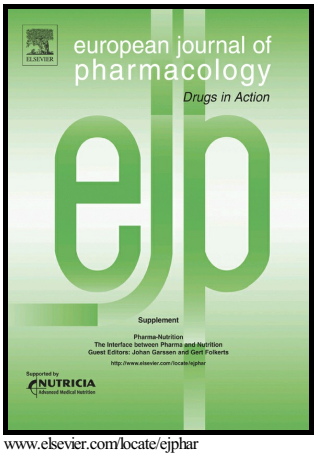

www.elsevier.com/locate/ejphar

Decarboxylation of Ang-(1–7) to Ala[1]-Ang-(1–7) leads to significant changes in pharmacodynamics

Anja Tetzner, Maura Naughton, Kinga Gebolys, Jenny Eichhorst, Esther Sala, Óscar Villacañas, Thomas Walther

PII: S0014-2999(18)30296-6
DOI: https://doi.org/10.1016/j.ejphar.2018.05.031
Reference: EJP71813

To appear in: *European Journal of Pharmacology*

Received date: 18 January 2018
Revised date: 18 May 2018
Accepted date: 18 May 2018

Cite this article as: Anja Tetzner, Maura Naughton, Kinga Gebolys, Jenny Eichhorst, Esther Sala, Óscar Villacañas and Thomas Walther, Decarboxylation of Ang-(1–7) to Ala[1]-Ang-(1–7) leads to significant changes in pharmacodynamics, *European Journal of Pharmacology,* https://doi.org/10.1016/j.ejphar.2018.05.031

Decarboxylation of Ang-(1-7) to Ala^{1}-Ang-(1-7) leads to significant changes in pharmacodynamics

Anja Tetzner[a,b*]; Maura Naughton[a*]; Kinga Gebolys[a]; **Jenny Eichhorst[c]**; Esther Sala[d]; Óscar Villacañas[d]; Thomas Walther[a,b,e]

*Equally contributing first authors

[a]Dept. Pharmacology and Therapeutics, School of Medicine and School of Pharmacy, University College Cork (UCC), Cork, Ireland;

[b]Departments Obstetrics and Paediatric Surgery, University of Leipzig, Leipzig, Germany;

[c]**Leibniz-Forschungsinstitut for Molekulare Pharmakologie (FMP), Berlin, Germany;**

[d]Intelligent Pharma, Barcelona, Spain;

[e]Institute of Medical Biochemistry and Molecular Biology, University Medicine Greifswald, Greifswald, Germany.

Corresponding Author: Prof. Thomas Walther, Department Pharmacology & Therapeutics, School of Medicine and School of Pharmacy, Western Gateway Building, Western Road, University College Cork, Cork, Ireland; Phone: +353-21-420-5973, fax: +353-21-4205471, E-mail: t.walther@ucc.ie

Abstract

The heptapeptide angiotensin (Ang)–(1-7) is part of the beneficial arm of the renin-angiotensin system. Ang-(1-7) has cardiovascular protective effects, stimulates regeneration, and opposes the often detrimental effects of Ang II. We recently identified the G protein-coupled receptors Mas and MrgD as receptors for the heptapeptide. Ala^1-Ang-(1-7) (Alamandine), a decarboxylated form of Ang-(1-7), has similar vasorelaxant effects, but has been described to only stimulate MrgD. Therefore, this study aimed to characterise the consequences of the lack of the carboxyl group in amino acid 1 on intracellular signalling and to identify the receptor fingerprint for Ala^1-Ang-(1-7).

In primary endothelial and mesangial cells, Ala^1-Ang-(1-7) elevated cAMP concentration. Dose response curves generated with Ang-(1-7) and Ala^1-Ang-(1-7) significantly differed from each other, with a much lower EC_{50} and a bell-shape curve for Ala^1-Ang-(1-7). We provided pharmacological proof that both, Mas and MrgD, are functional receptors for Ala^1-Ang-(1-7). Consequently, in primary mesangial cells with genetic deficiency in both receptors the heptapeptide failed to increase cAMP concentration. As we **previously described for Ang-(1-7), the Ala^1-Ang-(1-7)-**mediated cAMP increase **in Mas/MrgD-transfected HEK293 cells and primary cells were blocked by the AT2 receptor blocker, PD123319.** The very distinct dose-response curves for both heptapeptides could be explained by *in silico* modelling, electrostatic potential calculations, and an involvement of $G_{alpha\ i}$ for higher concentrations of Ala^1-Ang-(1-7).

Our results identify Ala^1-Ang-(1-7) as a peptide with specific pharmacodynamic properties and build the basis for the design of more potent and efficient Ang-(1-7) analogues for therapeutic interventions in a rapidly growing number of diseases.

Keywords : Ala^1-Angiotensin-(1-7), dose-response curve, G-proteins, Mas receptor, MrgD receptor, renin-angiotensin system

1. Introduction

The renin-angiotensin system consists of an increasing number of angiotensin (Ang) peptides which play an important role in the regulation of arterial blood pressure, electrolyte homeostasis, and water and sodium intake (Crowley et al., 2012), as well as in processes like tissue regeneration (Takeda et al., 2004, Wang et al., 2010). The renin-angiotensin system is a complex cascade in which precursor peptides are processed by specific enzymes to their active forms. In the past few years especially, Ang-(1-7) has become a peptide of interest, because of its beneficial actions in cardiovascular and renal diseases, counter-regulating the adverse effects of AngII (Mercure et al., 2008). Ang-(1-7) is mainly produced from AngII by Ang converting enzyme 2 (ACE2) (Vickers et al., 2002).

In previous work, we identified the G protein-coupled receptor Mas to be associated with Ang-(1-7)-induced signalling which could be blocked by D-Ala^{7}-Ang-(1-7), also named A779, a specific Ang-(1-7) antagonist (Santos et al., 2003). Very recently, we also discovered a second receptor for the heptapeptide, the Mas-related G protein-coupled receptor MrgD (Tetzner et al., 2016). In that study, we also showed that the primary intracellular pathway activated by Ang-(1-7) interactions with either Mas or MrgD involves adenylyl cyclase, cAMP and phosphokinase A (Tetzner et al., 2016).

A decade ago, Jankowski et al. identified a modified analogue of AngII in human plasma (Jankowski et al., 2007). This Ala^{1}-AngII, the authors named AngA, can be generated by the decarboxylation of the amino acid aspartate on position one to alanine. AngA interacts with the AT1 receptor (Yang et al., 2010) and its physiological effects can be blocked by the AT1 receptor blocker candesartan (Yang et al., 2011). Based on such findings, an international team hypothesized the existence of Ala^{1}-Ang-(1-7) as a product of Ala^{1}-AngII through conversion by ACE2 (Lautner et al., 2013). Indeed, Ala^{1}-Ang-(1-7) has been identified and named alamandine. As Kupchan et al. used similar terminology,

Allamandin, for a completely different molecule, we will use the original term, Ala^1-Ang-(1-7), describing the amino acid change in Ang-(1-7), to prevent confusion (Kupchan et al., 1974). Lautner et al. characterized Ala^1-Ang-(1-7) as the target peptide for the MrgD receptor but not for the Mas receptor (Lautner et al., 2013). However, as we could show that Ang-(1-7) can stimulate both Mas and MrgD, we aimed to test whether Ala^1-Ang-(1-7) targets the same receptors as Ang-(1-7), or shows a distinct receptor fingerprint. In particular, we focused on the characterisation of the ligand/receptor pharmacology, by determining efficiency and potency using receptor-transfected HEK293 cells, human endothelial cells, receptor-deficient primary mesangial cells, and a variety of receptor blockers and enzyme inhibitors.

2. Materials and Methods

2. 1 Materials

Angiotensin (Ang)-(1-7), Ala^1-Ang-(1-7), D-Ala^7-Ang-(1-7), and D-Pro^7-Ang-(1-7) were synthetized from Biosyntan (Berlin, Germany). HEK293, Forskolin, RPMI-1640, HEPES solution, Sodium pyruvate, Trtiton X-100 and trypsin/EDTA were purchased from Sigma Aldrich (St. Louise, Missouri, USA). DMEM, Fetal Bovine Serum (FBS) and **L-**glutamine were purchased from GIBCO (Life Technologies, Carlsbad, California, USA). PD123319 was from Parke-Davis Pharmaceutical Research (Detroit, Michigan, USA). **Pertussis toxin (**PTX**)** was from EMD Millipore (Billerica, MA, USA). Polyfect transfection reagent from Qiagen (Venlo, Limburg, Netherlands), and Pierce BCA Protein Assay Kit from Thermo Fisher Scientific (Waltham, Massachusetts, USA). **NF 023 was purchased from Tocris**

Bioscience (Bristol, United Kingdom). Direct cAMP ELISA kit was from Enzo Life Sciences Ltd. (Exeter, United Kingdom). HUVEC were purchased from LONZA (Basel, Switzerland).

2. 2 Animals

Mice deficient in Mas, MrgD (Walther et al., 1998, Zylka et al., 2005) and both Mas and MrgD (double knockout) (Tetzner et al., 2016) have been bred and housed in the animal facilities at UCC, Cork, Ireland. Animal studies are reported in compliance with the ARRIVE guidelines (Kilkenny et al., 2010, McGrath et al., 2015). Experiments performed conformed with the guidelines from Directive 2010/63/EU of the European Parliament on the protection of animals used for scientific purposes. Experiments involving animals have been approved by the local Animal Experimentation Ethics Committee (AEEC) in UCC, and also by the Health Products Regulatory Authority (HPRA).

2. 3 Cell culture conditions, transfection and stimulation

Human embryonic kidney (HEK-293) cells were cultured in DMEM medium supplemented with FBS (10%), HEPES buffer (1%), sodium pyruvate (1%), and L-glutamine (1%) and maintained under standard conditions (5% CO_2, 95 % humidity and 37º C). Cells were cultured in 100mm cell culture dishes and seeded in 48-well plates at a density of 75,000 cells per well. The next day, HEK-293 cells were transfected using a transient transfection procedure following the manufacturer's instructions. Briefly, 150ng of control plasmid pcDNA3.1 or a combination of 50ng of pcDNA3.1 and 100ng of expression vectors containing the cDNA for Mas or MrgD were mixed with serum-free medium and PolyFect

transfection reagent. After 10min incubation at room temperature, which allowed the complex formation, complete medium was added and the total volume was transferred into appropriate wells of the 48-well plate. The cells were incubated for 16-20h. The next day, the medium was replaced by serum-free medium 1h before stimulation. After stimulation with A779, D-Pro, PD123319, Forskolin (all 10^{-6}M), NF 023 ($5x10^{-6}$M) or PTX (50ng/ml) for 15min, the solvent, Ala^{1}-Ang-(1-7) or Ang-(1-7) (all in the mentioned concentrations) were added for 15min. Then, the cells were lysed by adding 180µl/well of 0.1M hydrochloric acid with 0.1% Triton X-100, and the lysates were stored at −80°C until cAMP measurement. The protein concentration was determined using Pierce BCA Protein Assay Kit according to the manufacturer's protocol (Thermo Fisher Scientific, Waltham, Massachusetts, USA).

For fluoresence imaging, HEK293 cells were grown to 80-90% confluence and transfected with Mas-mCherry or MrgD-GFP constructs as described above.

2. 4 Isolation and culture of primary cells and their stimulation

Kidney mesangial cells (MC) were isolated from 10-12-week old mice deficient in Mas and MrgD, and from their age- and gender-matched C57/BL6 control, according to the protocol previously described (Zhu et al., 2013). MC were cultured in 75cm^2 tissue culture flasks and seeded at passage 2 for stimulation in 24-well plates at a density of 100,000 cells per well.

Primary human umbilical vein endothelial cells (HUVEC) were purchased from LONZA (Basel, Switzerland). HUVEC were cultured in 100mm cell culture dishes and were seeded at 75,000 per well in 24-well plates at passage 5-7, for stimulation. Stimulation with Ala^{1}-Ang-(1-7) and the blockers was carried out as described above.

2. 5 Measurement of cAMP in cell lysates

cAMP concentration in cell lysates was determined using Direct cAMP ELISA kit (Enzo Life Sciences Ltd., Exeter, United Kingdom). Briefly, wells of 96-well plate (Goat Anti-Rabbit IgG pre-coated) were neutralized with 50µl of Neutralizing Reagent. Next, 100µl of acetylated cAMP standard or cell lysate was added, followed by 50µl of blue cAMP-Alkaline Phosphatase Conjugate and 50µl of yellow EIA Rabbit Anti-cAMP antibody. The plate was then incubated on a shaker (~ 400rpm) at room temperature for 2h. Next, the wells were aspirated and rinsed three times with Wash Buffer (1:10, Tris buffered saline containing detergents and sodium azide in deionized water). After the final wash, the plate was tapped against clean paper towel to remove any remaining Wash Buffer. To each well, 200µl p-Nitrophenyl Phosphate Substrate Solution was added, and the plate was incubated for 1h at room temperature. The enzymatic reaction was stopped by adding 50µl of Stop Solution, and the absorbance at 405 nm was measured immediately. The cAMP concentration was determined from non-linear standard curve using GraphPad Prism 6.0 software.

2. 6 mRNA isolation and real-time PCR

Total cellular RNA was isolated using the NucleoSpin RNA isolation kit (MACHEREY-NAGEL, Düren, Germany) according to the manufacturer's protocol. After isolation, 2,000ng total RNA was transcribed into cDNA using the RevertAid H Minus First Strand cDNA Synthesis kit (MBI Fermentas, Hanover, MD, USA) and oligo(dT)18 primer according to the manufacturer's guidelines. After synthesis, RNAse free water was added to the single cDNA to a final volume of 100µl. Quantification of mRNA levels was performed by real-time quantitative PCR (RT-PCR) on the StepOne™ Real-Time PCR System (Thermo Fisher

Scientific, Waltham, Massachusetts, USA) employing the Platinum SYBR Green qPCR SuperMix-UDG (Invitrogen) and gene specific primers (Mas forward: CCATCCTCAGCTTCTTGGTCTT, Mas reverse: TGGGAACCTGCATAACATCTCC, MrgD forward: AACAAACACCAGTGCTTCAAGG, MrgD reverse: CGTTTCACATCCACCCAGTAGA). The amplifications were performed in a final volume of 20µl using the following PCR cycle: 95°C for 15min followed by 40 cycles with denaturation at 95°C for 30s, annealing at 58°C for 30s and elongation at 72°C for 30s. PCR products were finally subjected to a melting curve analysis. The mRNA levels were quantified with the StepOne™ analysis software in comparative quantitation mode and normalized to beta-Actin expression levels. All quantitative RT-PCRs were performed at least three times in duplicate using RNA from independent experiments.

2. 7 In silico modelling

The 3-dimensional structure of Ang-(1–7) was prepared by minimizing their nuclear magnetic resonance experimental structures (PDB:2JP8) with Schrödinger Macromodel (MacroModel, version 9.7, Schrödinger, LLC, New York, NY), using AMBER94 force field and water solvent. It was further docked (keeping the backbone rigid) with Autodock 4.2.3 (Huey et al., 2007) into a modeled structure of the Mas receptor (Horn et al., 2003), in which the F112 side chain conformation was further modified to create a larger binding site and to expose specific binding residues (Perodin et al., 2002, Prokop et al., 2013). The complex was minimized as before. Surface areas and electrostatic potentials were computed with Schrödinger Maestro (Maestro, version 11.3.016, Release 2017-3, Platform Linux-x86_64, Schrödinger, LLC, New York, NY).

2. 8 Statistical Analyses

To ensure reproducibility of the results and to minimize bias, HEK293 cells, MC, and HUVECs were used at comparable passage numbers. The same kits and reagents were used for the experiments wherever possible. Data presented are mean ± S.E.M. where n denotes the number of experiments in triplicates. A *P*-value of <0.05 was considered statistically significant. Data were analysed with GraphPad Prism 6.0 (GraphPad Software Inc., San Diego, CA, USA) to produce dose-response curves using XY analyses with non-linear regression in a bell-shape fit. The EC_{50} and IC_{50} values were obtained using XY analyses with non-linear regression and the log (agonist or inhibitor) vs. response function. Statistical tests preformed were a Student's t-test or a one-way analysis of variance *(*ANOVA) tests accompanied by Bonferroni post hoc test.

3. Results

3.1 Ala[1]-angiotensin-(1-7) stimulates the generation of intracellular cAMP in endothelial cells

As we previously demonstrated that Ang-(1-7) can increase intracellular cAMP in a dose-dependent manner (Tetzner et al., 2016), we first tested whether Ala[1]-Ang-(1-7) can act in a similar manner using the most commonly characterized endothelial cell-line, human umbilical vein endothelial cells (HUVEC). Although Ala[1]-Ang-(1-7) was comparably as efficient as Ang-(1-7), the dose-response curve showed a completely different appearance (**Fig. 1A**). Not only is the curve bell-shaped in contrast to the one generated by Ang-(1-7)

which runs into a plateau with increasing concentrations, the increase in cAMP occurs much earlier with a leftward shift of almost 3 magnitudes of order (EC_{50} was reached at 3.6 x 10^{-11}M with Ala^1-Ang-(1-7) and at 1.1 x 10^{-8}M with Ang-(1-7)).

To investigate whether this effect on cAMP is mediated by receptors that are sensitive to the two Ang-(1-7) antagonists, A779 and D-Pro, and to the unspecific AT2 receptor blocker PD123319, which we identified as also blocking the Ang-(1-7) receptors Mas and MrgD (Tetzner et al., 2016), we used Ala^1-Ang-(1-7) in the concentration of highest efficacy (10^{-9}M) without and with the 3 receptor blockers **(10^{-6}M)**. As shown in Fig. 1B, the three compounds did not affect base-line cAMP concentrations, but all three blockers significantly reduced the increase in intracellular cAMP in response to Ala^1-Ang-(1-7) (**Fig. 1B**).

3.2 Ala^1-angiotensin-(1-7) stimulates the generation of intracellular cAMP in HEK293 cells expressing MrgD

Based on our work with Ang-(1-7) (Tetzner et al., 2016) and the results published by Lautner et al.,(Lautner et al., 2013), we then tested Mas- and MrgD-transfected cells. As shown in **Fig. 2A**, Ala^1-Ang-(1-7) stimulation caused a dose-dependent increase in the intracellular cAMP level in MrgD-transfected cells with an EC_{50} of 3.98 x 10^{-13}M. Since in HUVEC the dose-response curve peaked at 10^{-9}M of Ala^1-Ang-(1-7) but in MrgD-transfected cells at 10^{-11}M, we selected 10^{-11}M for further tests with the previously effective blockers. **Fig. 2B** shows that none of the 3 blockers had a baseline effect on cAMP levels in the pcDNA3.1 control or in MrgD-transfected cells. However, the increase in cAMP concentration generated by Ala^1-Ang-(1-7) in MrgD-transfected cells was blocked by D-Pro and PD123319, but not by A779 (**Fig. 2B**).

3.3 Ala[1]-angiotensin-(1-7) stimulates the generation of intracellular cAMP in HEK293 cells expressing Mas

In experiments with HEK293 cells transfected with the Mas receptor, Ala[1]-Ang-(1-7) also caused a dose-dependent increase in cAMP concentration with an EC_{50} value of **1.58×10^{-12}M** reaching highest efficacy at 5×10^{-11}M (**Fig. 2C**). In contrast to MrgD-transfected cells, D-Pro, PD123319 and A779 all blocked the Ala[1]-Ang-(1-7)-mediated increase in cAMP level in Mas-transfected cells (**Fig. 2D**).

3.4 Ala[1]-angiotensin-(1-7) in higher concentrations activates $G_{\alpha i}$, reducing the generation of cAMP

As cAMP is generated by the enzyme adenylyl cyclase which can be activated by $G_{\alpha s}$ but also inhibited by $G_{\alpha i}$ signalling, we hypothesised that the bell-shaped curve could be the result of a $G_{\alpha i}$ activation when using higher concentrations of Ala[1]-Ang-(1-7). We used MrgD receptor-transfected cells and generated dose-response curves for Ala[1]-Ang-(1-7) with and without pre-treatment with PTX, a $G_{\alpha i}$ inhibitor, which prevents the $G_{\alpha i}$ proteins from interacting with the receptor. Since the $G_{\alpha i}$ subunits remain locked in their inactive state, they are unable to inhibit adenylate cyclase activity. As shown in **Fig. 3A**, the parallel treatment with PTX prevented the decline in intracellular cAMP concentrations with increasing concentrations of Ala[1]-Ang-(1-7).

We then carried out identical experiments with PTX using Mas-transfected cells. As shown in Fig. 3B**, the parallel treatment with PTX also prevented the decline in intracellular cAMP level with higher concentration of Ala^1-Ang-(1-7), as seen for MrgD-transfected cells before (Fig. 3A).**

To confirm the PTX data, we used a second, selective $G_{\alpha i}$ inhibitor, NF 023 (Freissmuth et al., 1996). As for PTX, treatment with NF 023 prevented the decline in intracellular cAMP concentrations with increasing concentrations of Ala^1-Ang-(1-7) in both Mas and MrgD-transfected cells (Fig. 3C**).**

To confirm specific overexpression of mRNA for both receptors, we measured expression of receptor mRNA in MrgD and Mas-transfected cells to illustrate transfection efficacy. As shown in **Fig. 3D**, transfection with Mas or MrgD plasmids led to a significant overexpression of the receptor mRNA.

To visualise the transfection efficacy on protein level, HEK293 cells were transfected with Mas-mCherry or MrgD-GFP as seen in Fig. 3E**. In transfected cells carrying the receptor cDNA, both receptors are expressed in the cytoplasmic membranes of these cells.**

3.5 Absence of Ala^1-angiotensin-(1-7)-mediated cAMP generation in mesangial cells derived from Mas/MrgD knockout animals

To test whether the lack of Mas and MrgD blunts the ability of Ala^1-Ang-(1-7) to generate cAMP in primary mesangial cells, as previously examined in Ang-(1-7), we used mesangial cells derived from double knockout mice deficient in both receptors, a strain introduced recently (Tetzner et al., 2016). Ala^1-Ang-(1-7) increased cAMP dose-dependently in wild-

type mesangial cells **(EC_{50} = 5.37 X 10^{-13}M)** with a typical bell-shape curve as shown before in endothelial cells, and Mas or MrgD-transfected HEK cells. (**Fig. 4A**). While D-Pro, PD123319 and A779 did not affect base-line cAMP concentrations in mesangial cells, all three compounds blocked the Ala^1-Ang-(1-7)-mediated increase in cAMP level in these wild-type cells (**Fig. 4B**). This cAMP increase observed in wild-type mesangial cells was completely blunted in mesangial cells isolated from double-knockout mice (**Fig. 4C**). In addition, Forskolin, a direct adenylyl cyclase activator, increased cAMP concentration in DKO mesangial cells, illustrating that the lack of stimulation by Ala^1-Ang-(1-7) is not based on a general inefficacy of the cells to generate cAMP in response to stimulation.

Next, we tested whether the Ala^1-Ang-(1-7)-mediated increase in cAMP observed in WT mesangial cells could be abolished in Mas or MrgD KO cells or whether it required deficiency in both receptors. Knockout in one of the receptors did not significantly reduce the Ala^1-Ang-(1-7) signal generated in wild-type cells, while the double knockout again completely blunted the effect (Fig. 4D**).**

3.6 In silico *modelling to explain the differences in potency between Ala^1-angiotensin-(1-7)-and angiotensin-(1-7)*

The proposed binding mode of Ang-(1-7) places Arg^2 in a position to establish a salt bridge with Glu^{167} and a cation-π interaction with Tyr^{248} of the Mas receptor. These interactions constrain the mobility of the N-terminal part of Ang-(1-7) and prevent the negatively charged carboxylate in Asp^1 side chain from interacting with a positive chemical group in the protein (see Fig. 5A**, where Arg^{181} and Arg^{185} of Mas receptor are explicitly shown, as they are the closest positively charged residues to Ang-(1-7)). Actually, the electrostatic potential surface of the binding site is estimated with a**

positive surface area value of 5 Å^2 and a much greater negative surface area value of 109 Å^2 (considering residues within 5 Å of Ang-(1-7)). This predominance of a negatively charged protein surface is more stressed on the extracellular side (where the N-terminal Ang-(1-7) is predicted to bind), as seen in Fig. 5A. Fig. 5B shows the complementarity between the electrostatic potential surfaces of both Ang-(1-7) and the receptor. There is a close contact of non-complementary areas around the side chains of Asp^1 of Ang-(1-7) and Asp^{173} of the receptor. This is mainly due to the proximity of negatively charged areas. The fact that Ala^1-Ang-(1-7) does not have a negatively charged carboxylate group in the first residue may stabilise its interactions with the receptor and, thus, could be a reason for its greater potency in comparison to Ang-(1-7).

4. Discussion

Here, we demonstrate that Ala^1-Ang-(1-7), like Ang-(1-7), stimulates the generation of the second messenger, cAMP, and cAMP is thus an ideal tool to quantify changes in intracellular signalling mediated by Ala^1-Ang-(1-7). Using this readout allowed us to provide final pharmacological evidence that MrgD is a functional receptor for Ala^1-Ang-(1-7). More importantly, the use of cAMP as a readout enabled us to generate results providing the first experimental proof that Mas is the second receptor for Ala^1-Ang-(1-7). Furthermore, our data confirm findings with Ang-(1-7) (Tetzner et al., 2016), that A779 fails to significantly reduce the stimulation of cAMP production by Ala^1-Ang-(1-7) in MrgD-transfected cells. This may be due to the D-orientation of alanine in position 7, which might prevent the peptide fitting into the MrgD receptor, while it still fits into Mas and thus, can block the agonist effects there.

Previous work by other groups implicated that the two Ang peptides, Ang-(1-7) and Ala^1-Ang-(1-7) target different receptors, with Ala^1-Ang-(1-7) stimulating MrgD but not Mas (Lautner et al., 2013). Our data shows that not only can Ang-(1-7) can signal via Mas and MrgD, but also the decarboxylated version of the heptapeptide, Ala^1-Ang-(1-7). One of the reasons for this discrepancy might be due to our finding that Ala^1-Ang-(1-7) generates a bell-shaped dose response curve and is much more potent than Ang-(1-7). Consequently, at concentrations where Ang-(1-7) is most efficient, Ala^1-Ang-(1-7) might have little effect as it is back to base-line levels of cAMP. However, since we measured cAMP, while others looked on NO release, it would be interesting to see whether increasing concentrations of Ala^1-Ang-(1-7) would also generate a dose-response curve for NO, with highest efficiency similar to the EC_{50} described here for receptor-transfected cells and primary kidney and endothelial cells. Nevertheless, our findings are also supported by modelling of Ang-(1-7) in the Mas receptor binding site, in which the decarboxylation of the first residue could lead to a more favorable electrostatic complementary with the receptor surface and thus, making it likely that the Mas receptor could also be a receptor for Ala^1-Ang-(1-7).

While our data excludes a receptor fingerprint discriminating between both peptides, one of the key findings of our experiments is that Ala^1-Ang-(1-7) is much more potent than Ang-(1-7), although the difference between both peptides seems marginal, with only a lack of the carboxylate group in Ala^1-Ang-(1-7).

To better understand the reason for improved potency, we investigated the potential binding mode of the N-terminal segment of Ang-(1-7), as well as the electrostatic potential of the binding site and its complementarity to Ang-(1-7). Our predictions show how the Asp^1 side chain may not be stabilised due to a charge repulsion with the highly negatively charged surface of the receptor, although the water accessibility of this area could screen this effect (screening is the damping of electric fields). The fact that Ala^1-Ang-(1-7) does not have the

carboxylate group in the first residue, thus avoiding a potential charge repulsion with the predominantly negatively charged area, may be a reason for its observed increased potency. In addition, this same absence may favour a salt bridge between the N-terminal amino group and the Mas receptor, particularly with Asp^{173}. Thus, the interactions extracted from this model might build the base for a screening program to identify agonists stimulating Mas and MrgD.

Another very dominant pharmacodynamic difference between the two peptides is the bell-shaped dose-response curve for Ala^1-Ang-(1-7). There are hints in the literature, which might explain this bell-shaped dose-response curve. Since the late nineties, different groups have shown the ß2-adrenergic receptor to couple not only to $G_{\alpha s}$, but also to $G_{\alpha i}$ proteins in the heart (Xiao et al., 1995, Xiao et al., 1999) and in receptor-transfected HEK293 cells (Daaka et al., 1997), whereby the degree of activation of the two G proteins would define the agonist effect on intracellular cAMP concentrations. Interestingly, it has been also shown that this dual activation is not specific for the ß2-adrenergic receptor but has also been seen in histamine, serotonin, and glucagon receptors (Kilts et al., 2000).

A decade ago, Beyermann et al. (Beyermann et al., 2007) confirmed this model by using the corticotropin-releasing factor receptor type 1. They demonstrated that native ligands stimulated $G_{\alpha i}$ and $G_{\alpha s}$ proteins, whereby in all cases, $G_{\alpha i}$.has been activated approx. two magnitudes of order to the right. Therefore, we tested whether Ala^1-Ang-(1-7) could also lead to an $G_{\alpha i}$ activation in higher concentrations, reducing the $G_{\alpha s}$-mediated increase in cAMP. By using PTX, a substance that prevents $G_{\alpha i}$-associated inhibition of adenylyl synthase leading to a reduction in intracellular cAMP, the decline in the dose response curve observed with Ala^1-Ang-(1-7) alone, disappeared. The curve runs in a plateau following PTX treatment and looked similar to the Ang-(1-7) curve, although with a significant leftward shift. Thus, it

looks like Ala^1-Ang-(1-7), but not Ang-(1-7) can activate two G proteins, and thus, similar to a car, by pressing the gas and brake pedal, it brings the speed (an increase in cAMP) to zero.

The authors are aware that limitations of our study include the lack of knowledge in whether the decarboxylation of Ang-(1-7) to Ala^1-Ang-(1-7) results in any loss or gain of funcion *in vivo,* which can only be evaluated by animal and human studies. However, the enzyme being responsible for the reaction is still unidentified and thus, its inhibition / knockout *in vivo* can still not be experimentally realized.

Taken together, our results change the view on Ala^1-Ang-(1-7) as a peptide exclusively activating MrgD but not Mas, illustrate that minor changes in Ang-(1-7) (decarboxylation on amino acid 1) can lead to major changes in the response of both receptors and provide a mechanistic explanation for such differences. Thus, **by considering the structural differences in Ala^1-Ang-(1-7) and the resulting improvement in potency,** our data lays the foundation for the development of new Ang-(1-7) analogues which may generate a more potent stimulation of the receptors and hence, leading to safer and more efficient treatment options for a growing number of diseases in which Ang-(1-7) might be beneficial, based on its success in preclinical disease models.

Author Contributions

Anja Tetzner performed part of experiments for Fig. 1-4, developed the images for the figures and worked on the manuscript.

Maura Naughton performed part of experiments for Fig. 1-4 and worked on the manuscript.

Kinga Gebolys performed part of the experiments for Fig. 1A and 1B.

Jenny Eichhorst performed the imaging for Fig. 3E.

Esther Sala computed and analysed the electrostatic potential for Fig. 5.

Óscar Villacañas analysed the ligand-protein interactions for Fig. 5 and supervised the modelling work.

Thomas Walther initiated the work, coordinated the experiments, advised, drafted the main text body, and finalized the manuscript.

Financial Support

The work was supported by grants of the Deutsche Forschungsgemeinschaft (WA1441/22-1 and 2).

Disclosures

TW is inventor of the patent "Use of an Ang-(1-7) receptor agonist in acute lung injury" (Application No: 08016142.5-2107). TW is scientific advisor of Tarix Pharmaceuticals LTD (Boston, USA).

References

Beyermann M, Heinrich N, Fechner K, Furkert J, Zhang W, Kraetke O, Bienert M and Berger H (2007). Achieving signalling selectivity of ligands for the corticotropin-releasing factor type 1 receptor by modifying the agonist's signalling domain. *Br J Pharmacol* **151**(6): 851-859.

Crowley SD and Coffman TM (2012). Recent advances involving the renin-angiotensin system. *Exp Cell Res* **318**(9): 1049-1056.

Daaka Y, Luttrell LM and Lefkowitz RJ (1997). Switching of the coupling of the beta2-adrenergic receptor to different G proteins by protein kinase A. *Nature* **390**(6655): 88-91.

Freissmuth M, Boehm S, Beindl W, Nickel P, Ijzerman AP, Hohenegger M and Nanoff C (1996). Suramin analogues as subtype-selective G protein inhibitors. *Mol Pharmacol* 49(4): 602-611.

Horn F, Bettler E, Oliveira L, Campagne F, Cohen FE and Vriend G (2003). GPCRDB information system for G protein-coupled receptors. *Nucleic Acids Res* **31**(1): 294-297.

Huey R, Morris GM, Olson AJ and Goodsell DS (2007). A semiempirical free energy force field with charge-based desolvation. *J Comput Chem* **28**(6): 1145-1152.

Jankowski V, Vanholder R, Van Der Giet M, Tolle M, Karadogan S, Gobom J, Furkert J, Oksche A, Krause E, Tran TN, Tepel M, Schuchardt M, Schluter H, Wiedon A, Beyermann M, Bader M, Todiras M, Zidek W and Jankowski J (2007). Mass-spectrometric identification of a novel angiotensin peptide in human plasma. *Arteriosclerosis, thrombosis, and vascular biology* **27**(2): 297-302.

Kilkenny C, Browne W, Cuthill IC, Emerson M, Altman DG and Group NCRRGW (2010). Animal research: reporting in vivo experiments: the ARRIVE guidelines. *Br J Pharmacol* **160**(7): 1577-1579.

Kilts JD, Gerhardt MA, Richardson MD, Sreeram G, Mackensen GB, Grocott HP, White WD, Davis RD, Newman MF, Reves JG, Schwinn DA and Kwatra MM (2000). Beta(2)-adrenergic and several other G protein-coupled receptors in human atrial membranes activate both G(s) and G(i). *Circ Res* **87**(8): 705-709.

Kupchan SM, Dessertine AL, Blaylock BT and Bryan RF (1974). Isolation and structural elucidation of allamandin, an antileukemic iridoid lactone from Allamanda cathartica. *The Journal of organic chemistry* **39**(17): 2477-2482.

Lautner RQ, Villela DC, Fraga-Silva RA, Silva N, Verano-Braga T, Costa-Fraga F, Jankowski J, Jankowski V, Sousa F and Alzamora A (2013). Discovery and Characterization of Alamandine A Novel Component of the Renin–Angiotensin System. *Circulation research* **112**(8): 1104-1111.

Lautner RQ, Villela DC, Fraga-Silva RA, Silva N, Verano-Braga T, Costa-Fraga F, Jankowski J, Jankowski V, Sousa F, Alzamora A, Soares E, Barbosa C, Kjeldsen F, Oliveira A, Braga J, Savergnini S, Maia G, Peluso AB, Passos-Silva D, Ferreira A, Alves F, Martins A, Raizada M, Paula R, Motta-Santos D, Klempin F, Pimenta A, Alenina N, Sinisterra R, Bader M, Campagnole-Santos MJ and Santos RA (2013). Discovery and characterization of alamandine: a novel component of the renin-angiotensin system. *Circ Res* **112**(8): 1104-1111.

Mcgrath JC and Lilley E (2015). Implementing guidelines on reporting research using animals (ARRIVE etc.): new requirements for publication in BJP. *Br J Pharmacol* **172**(13): 3189-3193.

Mercure C, Yogi A, Callera GE, Aranha AB, Bader M, Ferreira AJ, Santos RA, Walther T, Touyz RM and Reudelhuber TL (2008). Angiotensin (1-7) blunts hypertensive cardiac remodeling by a direct effect on the heart. *Circulation research* **103**(11): 1319-1326.

Perodin J, Deraet M, Auger-Messier M, Boucard AA, Rihakova L, Beaulieu ME, Lavigne P, Parent JL, Guillemette G, Leduc R and Escher E (2002). Residues 293 and 294 are ligand contact points of the human angiotensin type 1 receptor. *Biochemistry* **41**(48): 14348-14356.

Prokop JW, Santos RA and Milsted A (2013). Differential mechanisms of activation of the Ang peptide receptors AT1, AT2, and MAS: using in silico techniques to differentiate the three receptors. *PLoS One* **8**(6): e65307.

Santos RAS, E Silva ACS, Maric C, Silva DMR, Machado RP, De Buhr I, Heringer-Walther S, Pinheiro SVB, Lopes MT, Bader M, Mendes EP, Lemos VS, Campagnole-Santos MJ, Schultheiss H-P, Speth R and Walther T (2003). Angiotensin-(1–7) is an endogenous ligand for the G protein-coupled receptor Mas. *Proceedings of the National Academy of Sciences of the United States of America* **100**(14): 8258-8263.

Takeda H, Katagata Y, Hozumi Y and Kondo S (2004). Effects of angiotensin II receptor signaling during skin wound healing. *Am J Pathol* **165**(5): 1653-1662.

Tetzner A, Gebolys K, Meinert C, Klein S, Uhlich A, Trebicka J, Villacanas O and Walther T (2016). G-Protein-Coupled Receptor MrgD Is a Receptor for Angiotensin-(1-7) Involving Adenylyl Cyclase, cAMP, and Phosphokinase A. *Hypertension* **68**(1): 185-194.

Vickers C, Hales P, Kaushik V, Dick L, Gavin J, Tang J, Godbout K, Parsons T, Baronas E and Hsieh F (2002). Hydrolysis of biological peptides by human angiotensin-converting enzyme-related carboxypeptidase. *Journal of Biological Chemistry* **277**(17): 14838-14843.

Walther T, Balschun D, Voigt JP, Fink H, Zuschratter W, Birchmeier C, Ganten D and Bader M (1998). Sustained long term potentiation and anxiety in mice lacking the Mas protooncogene. *J Biol Chem* **273**(19): 11867-11873.

Wang Y, Qian C, Roks AJ, Westermann D, Schumacher SM, Escher F, Schoemaker RG, Reudelhuber TL, Van Gilst WH, Schultheiss HP, Tschope C and Walther T (2010). Circulating rather than cardiac angiotensin-(1-7) stimulates cardioprotection after myocardial infarction. *Circulation. Heart failure* **3**(2): 286-293.

Xiao RP, Avdonin P, Zhou YY, Cheng H, Akhter SA, Eschenhagen T, Lefkowitz RJ, Koch WJ and Lakatta EG (1999). Coupling of beta2-adrenoceptor to Gi proteins and its physiological relevance in murine cardiac myocytes. *Circ Res* **84**(1): 43-52.

Xiao RP, Ji X and Lakatta EG (1995). Functional coupling of the beta 2-adrenoceptor to a pertussis toxin-sensitive G protein in cardiac myocytes. *Mol Pharmacol* **47**(2): 322-329.

Yang R, Smolders I, Vanderheyden P, Demaegdt H, Van Eeckhaut A, Vauquelin G, Lukaszuk A, Tourwe D, Chai SY, Albiston AL, Nahmias C, Walther T and Dupont AG (2011). Pressor and renal hemodynamic effects of the novel angiotensin A peptide are angiotensin II type 1A receptor dependent. *Hypertension* **57**(5): 956-964.

Yang R, Walther T, Gembardt F, Smolders I, Vanderheyden P, Albiston AL, Chai SY and Dupont AG (2010). Renal vasoconstrictor and pressor responses to angiotensin IV in mice are AT1a-receptor mediated. *Journal of hypertension* **28**(3): 487-494.

Zhu X, Wang Y, Schwiebs A and Walther T (2013). Chimeric natriuretic peptide ACNP stimulates both natriuretic peptide receptors, the NPRA and NPRB. *Mol Cell Endocrinol* **366**(1): 117-123.

Zylka MJ, Rice FL and Anderson DJ (2005). Topographically distinct epidermal nociceptive circuits revealed by axonal tracers targeted to Mrgprd. *Neuron* **45**(1): 17-25.

Figure Legends

Fig. 1: Intracellular cAMP is increased by Ala^1-Angiotensin-(1-7) in human umbilical vein endothelial cells (HUVEC). (A) HUVEC were stimulated for 15min with a range of concentrations (10^{-6} to 10^{-13}M) of Ala^1-Ang-(1-7) before analysis of cAMP concentration. (B) HUVEC were stimulated for 15min with blockers (A779, D-Pro^7-Ang-(1-7) (D-Pro) and PD123319 (all 10^{-6} M)), followed by 15min stimulation with Ala^1-Ang-(1-7) (10^{-9} M). Results are expressed as mean ± S.E.M.; (A) n=3, (B) n=4. Data was reported as a fold change or percentage of the untreated control mean. ***P<0.001, significantly different from control; $^{###}P$<0.001, $^{##}P$<0.01 or $^{#}P$<0.05, significantly different from Ala^1-Ang-(1-7); ANOVA with Bonferoni post-hoc test.

Fig. 2: Ala^1-Ang-(1-7) signals through MrgD and Mas receptors. (A) MrgD-transfected HEK293 cells were stimulated for 15min with a range of concentrations (10^{-6} to 10^{-18}M) of Ala^1-Ang-(1-7) before analysis of cAMP concentration. (B) Cells were stimulated for 15min with blockers (A779, D-Pro^7-Ang-(1-7) (D-Pro) and PD123319 (all 10^{-6}M)), followed by 15min stimulation with Ala^1-Ang-(1-7) (10^{-11}M). (C) Mas-transfected HEK293 cells were stimulated for 15min with a range of concentrations (10^{-6} to 10^{-18}M) of Ala^1-Ang-(1-7) before analysis of cAMP concentration. (D) Cells were stimulated for 15min with blockers (all 10^{-6}M)), followed by 15min stimulation with Ala^1-Ang-(1-7) (10^{-11}M). Results are expressed as mean ± S.E.M.; (A) n=4, (B) n=5, (C) n=6 and (D) n=5. Data was reported as a fold change or percentage of the untreated control mean. ***P<0.001, significantly different from the MrgD control; $^{###}P$<0.001, significantly different from Ala^1-Ang-(1-7); ANOVA with Bonferoni post-hoc test.

Fig. 3: Ala^1-Ang-(1-7) in higher concentrations activates $G_{\alpha i}$. (A) MrgD-transfected HEK293 cells were stimulated for 15min with PTX (50ng/ml) followed by stimulation with Ala^1-Ang-(1-7) (10^{-11}M) for a further 15min. **(B) Mas-transfected HEK293 cells were stimulated with PTX, followed by stimulation with 3 doses of Ala^1-Ang-(1-7) ($10^{-7,}$ 10^{-11} & 10^{-14}M) for a further 15min. (C) HEK293 cells were stimulated for 15min with NF 023 ($5x10^{-6}$M) followed by stimulation with 3 doses of Ala^1-Ang-(1-7) ($10^{-7,}$ 10^{-11} & 10^{-14}M) for a further 15min.** (D) mRNA of Mas and MrgD-transfected HEK293 cells (pcDNA3.1 values are set as 1). **(E) Fluorescence microscopy of HEK293 cells transfected with Mas-mCherry (red) and MrgD-GFP (green).** Results are expressed as mean ± S.E.M.; (A) n=4, (B) n=2, (C) n=3 and (D) n=6. Data was reported as a fold change or percentage of the untreated control. ***P<0.001, **P<0.01, significantly different from pcDNA3.1 control; $^{\#\#\#}P$<0.001, significantly different from Ala^1-Ang-(1-7) 10^{-7}M; $^{\$\$}P$<0.01, $^{\$\$\$}P$<0.001, significantly different from Ala^1-Ang-(1-7) 10^{-14}M; ANOVA with Bonferoni post-hoc test and Students T-test.

Fig. 4: Ala^1-Ang-(1-7) induced signalling is absent in mesangial cells derived from Mas/MrgD double-knockout animals. (A) WT C57BL/6 mesangial cells were stimulated for 15min with a range of concentrations (10^{-6} to 10^{-14}M) of Ala^1-Ang-(1-7) before analysis of cAMP concentration. (B) WT C57BL/6 mesangial cells were stimulated for 15min with blockers (A779, D-Pro^7-Ang-(1-7) (D-Pro) and PD123319 (all 10^{-6}M)), followed by 15min stimulation with Ala^1-Ang-(1-7) (10^{-11}M). (C) Mas/MrgD knockout (DKO) mesangial cells were stimulated for 15min with blockers (A779, D-Pro^7-Ang-(1-7) (D-Pro) and PD123319 (all 10^{-6}M)), followed by 15min stimulation with Ala^1-Ang-(1-7) (10^{-11}M). **(D) WT, Mas KO, MrgD KO and DKO mesangial cells were stimulated for 15min with Ala^1-Ang-(1-7) (10^{-11}M).** Results are expressed as mean ± S.E.M.; (A) n=6, (B) n=5, (C) n=2 and (D) n=

2-5. Untreated control values of each genotype is set as 100%. ***P<0.001, *P<0.05, significantly different from control mean; $^{###}P$<0.001, $^{\#}P$<0.05, significantly different from Ala^{1}-Ang-(1-7); ANOVA with Bonferoni post-hoc test.

Fig. 5: Electrostatic potential in Mas receptor binding site model. (A) Electrostatic potential of Mas receptor model, considering residues within 10 Å of the predicted binding pose of Ang-(1-7). (B) Electrostatic potential of Ang-(1-7) peptide in its predicted binding pose (solid surface) and Mas receptor model (mesh surface), considering residues within 3 Å of Ang-(1-7). Red areas are favourable to interact with positively charged groups and blue ones with negatively charged groups. Predicted binding pose of Ang-(1-7) is depicted in green-coloured carbon atoms. Ang-(1-7) residue labels are shown in italic type.

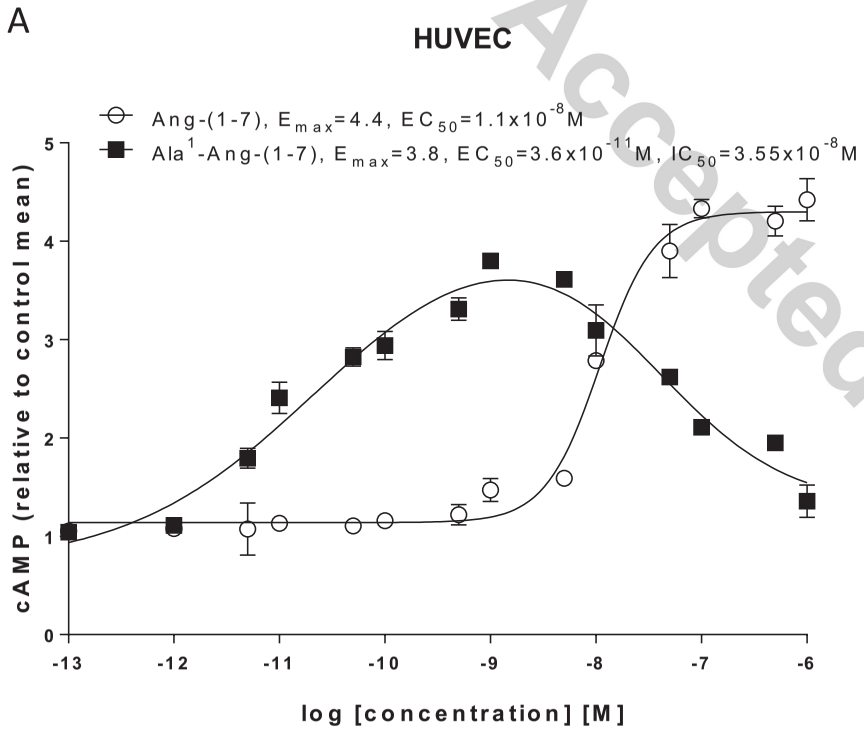

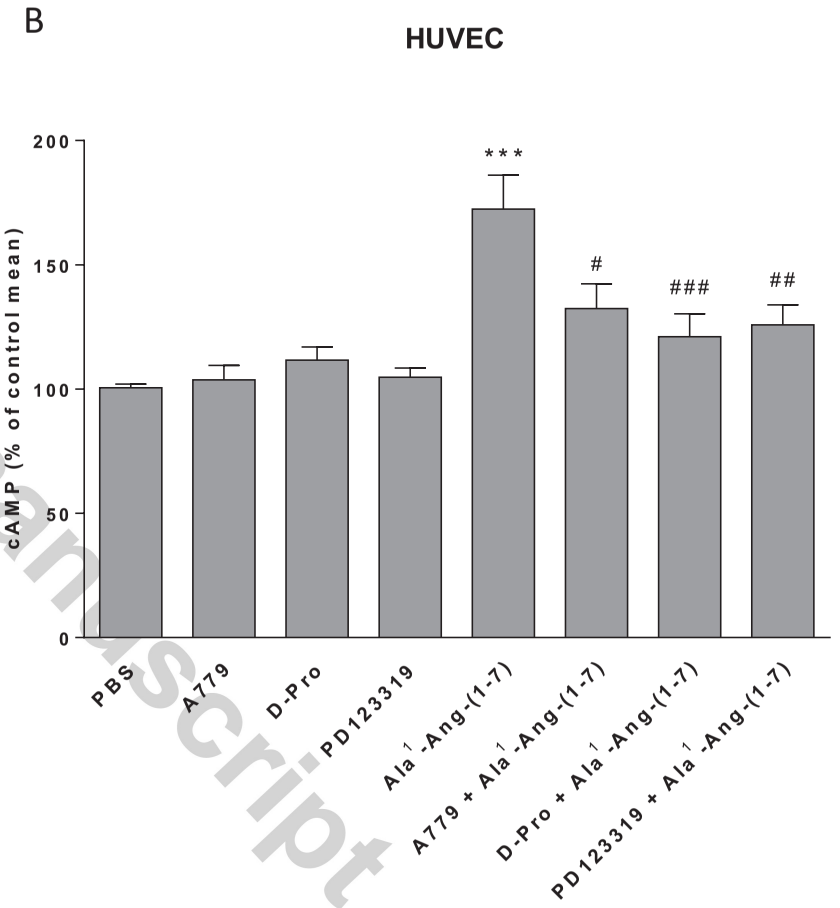

Figure 2

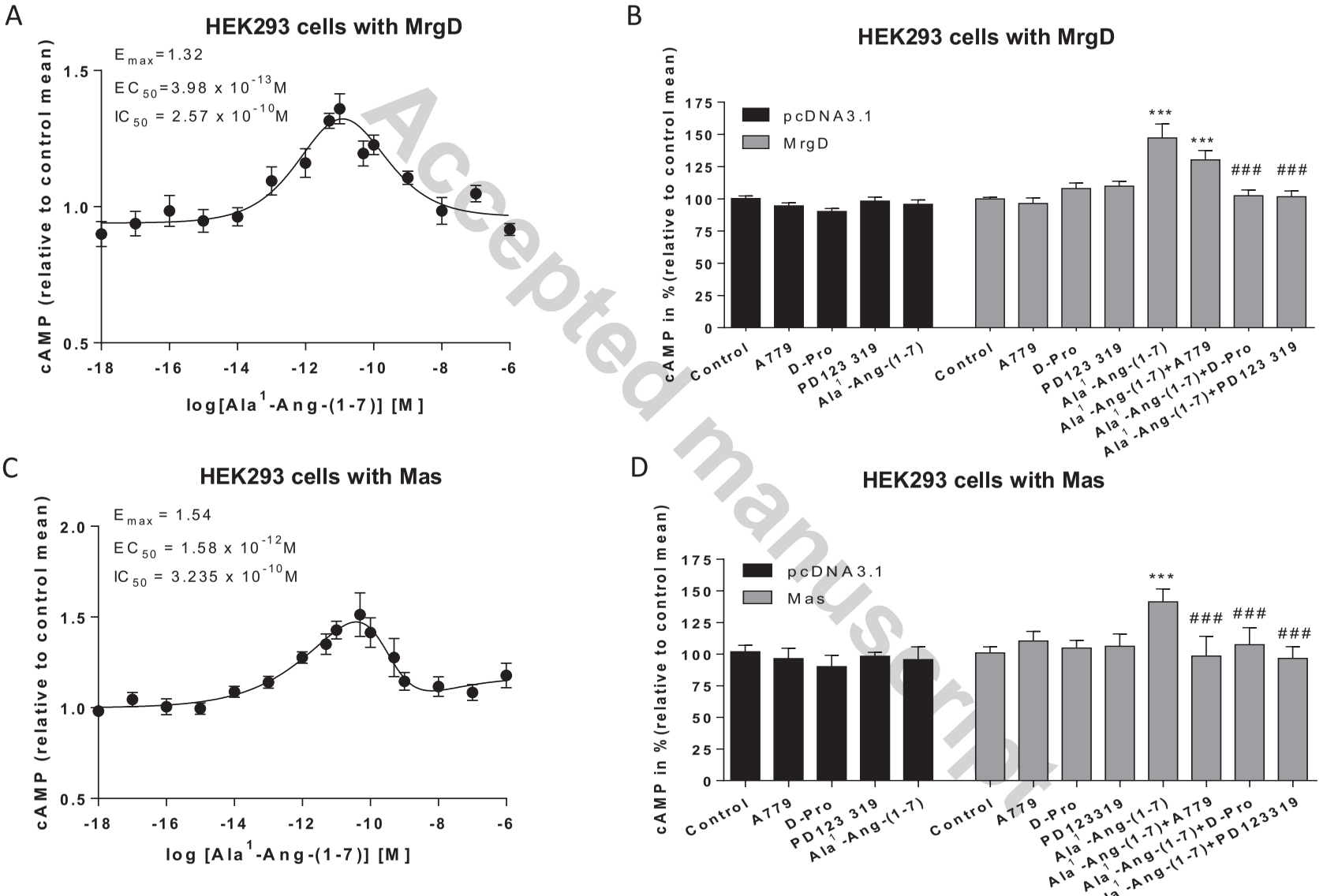

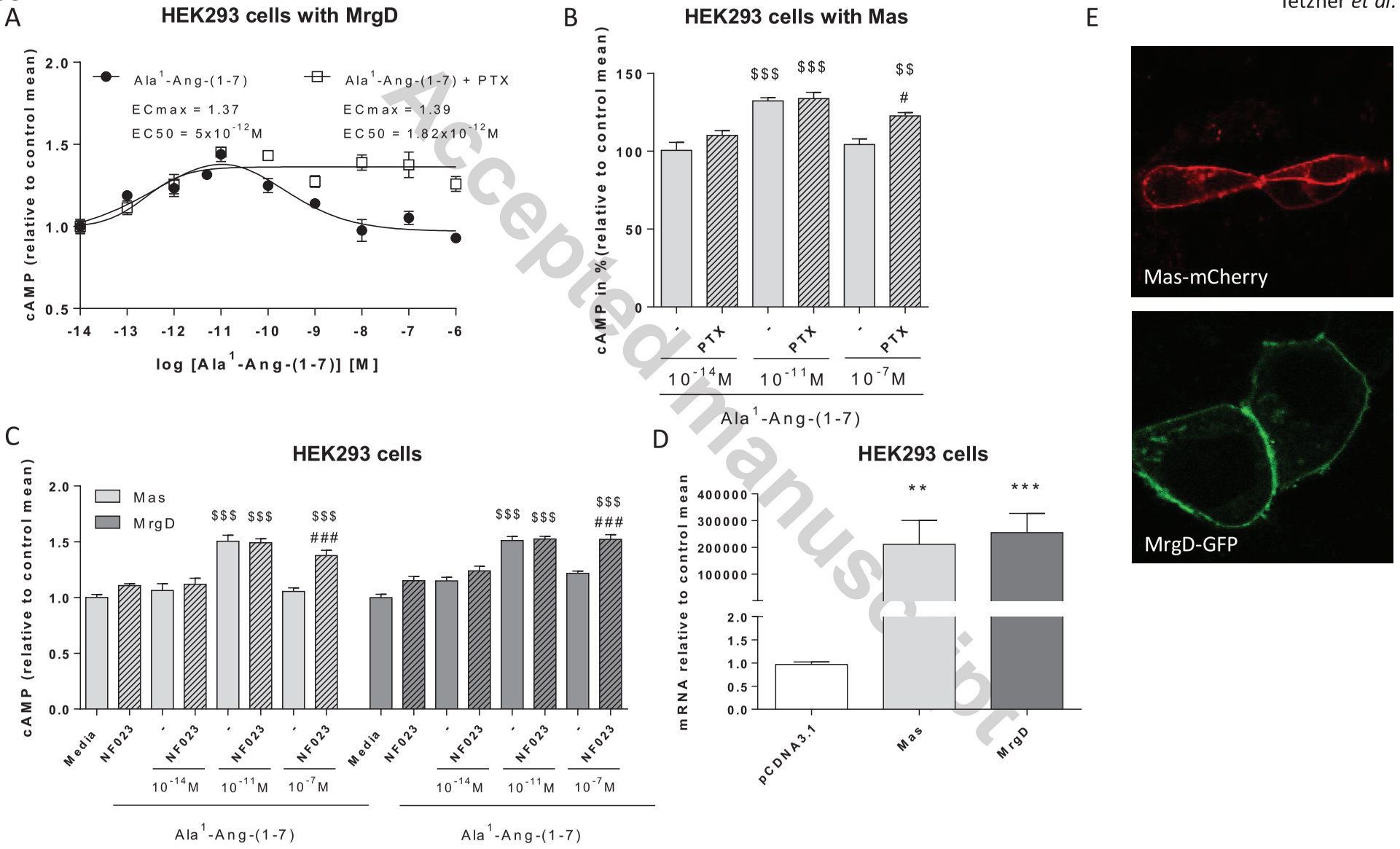

Figure 4